Available online at www.sciencedirect.com
ScienceDirect
Polymer 47 (2006) 7222–7230
polymer
www.elsevier.com/locate/polymer

Relaxation in poly(alkyl methacrylate)s: Change of intermolecular coupling with molecular structure, tacticity, molecular weight, copolymerization, crosslinking, and nanoconfinement

K.L. Ngai [a,*], T.R. Gopalakrishnan [b], M. Beiner [b]

[a] *Naval Research Laboratory, Washington, DC 20375-5320, USA*
[b] *Fachbereich Physik, Universität Halle, D-06099 Halle (Saale), Germany*

Received 30 January 2006; received in revised form 25 May 2006; accepted 7 June 2006
Available online 23 August 2006

Abstract

The voluminous amount of data in the literature on the structural α- and the Johari–Goldstein β-relaxations of the poly(*n*-alkyl methacrylate)s allows a systematic study of the interrelation between the two important relaxation processes. The data bring out the systematic changes in the interrelation between the structural α- and the Johari–Goldstein β-relaxations with changes in molecular structure, molecular weight, tacticity and size (by nanoconfinement), and modifications by copolymerization, and crosslinking. The results can all be interpreted as primarily due to changes in intermolecular coupling, which have significant effects on the many-molecule dynamics constituting the structural α-relaxation, but not on the precursory Johari–Goldstein β-relaxation. Theoretically, the Coupling Model predicts a relation of intermolecular coupling (or degree of cooperativity of the α-relaxation) to the ratio of the α- and the β-relaxation times, and a correlation of intermolecular coupling to the steepness or ''fragility'' index. The predicted relation and correlation are compared with experimental data of the poly(alkyl methacrylate)s.

Keywords: Poly(*n*-alkyl methacrylate); Glass transition; Johari–Goldstein relaxation

1. Introduction

A worthwhile effort in the research of relaxation in polymers is to understand the observed changes with molecular structure, and various manipulations of the chemical and physical structures. The results will benefit the ultimate understanding of the mechanisms of various relaxation processes found in polymers, which is important in both basic research and technological applications of this important class of materials. Pakula had contributed a great deal to our current understanding of the dynamics of polymers by his various research activities, which include his innovative methods of computer simulations and experimental measurements of many different polymers during his service at the Max-Planck-Institut für Polymerforschung and at the University of Łodz. Examples of his recent works are given in Refs. [1–5]. In this paper, we revisit a family of polymers, in some of which, namely isotactic and atactic poly(*n*-ethyl methacrylates) (PEMA), Pakula had made mechanical measurements just a couple of years before he passed away [6]. The family consists of the poly(*n*-alkyl methacrylates) (P*n*AMA). They have a polar backbone and flexible nonpolar side groups of different lengths, and offer an opportunity for such study [7]. Many different chemical and physical modifications can be made by varying the length of the side chain, the molecular weight, and the tacticity [7]. Other means include random copolymerization, plasticization by the addition of a diluent [7], and nanoconfinement in the form of ultrathin films [8]. For the special case of poly(*n*-hexyl methacrylate) (P*n*HMA), its structure can be modified to become poly(cyclohexyl methacrylate) (PCHMA) [9–13]. The poly(alkyl methacrylate)s all have a prominent secondary β-relaxation with properties indicating that it is the Johari–Goldstein (JG) [14–16] relaxation

* Corresponding author. Tel.: +1 202 767 6150; fax: +1 202 767 0546.
E-mail address: ngai@estd.nrl.navy.mil (K.L. Ngai).

0032-3861/$ - see front matter © 2006 Elsevier Ltd. All rights reserved.
doi:10.1016/j.polymer.2006.06.072

[17–22] and the precursor of the primary α-relaxation. By now, the literature has a voluminous amount of experimental results of the influence on the α- and the JG β-relaxations in the poly(alkyl methacrylate)s by these chemical and physical modifications [7,22]. The data offer plenty of opportunities and challenges for theoretical interpretation and explanation. The objective of this study is to collectively discuss these experimental data and interpret them by the original Coupling Model (CM) [23] and the extended version [24–27] that makes connection of its primitive relaxation time with the JG β-relaxation. The CM is particularly suitable for this task because it addresses both the α- and the β-relaxations, and the relation between them. From the ratio of the α- and the JG β-relaxation times, the CM is able to deduce the inherent intermolecular cooperativity or coupling of the α-relaxation. Hence we can see systematically how intermolecular cooperativity changes in the poly(alkyl methacrylate) series, and for a particular poly(alkyl methacrylate) how intermolecular cooperativity changes by various chemical and physical modifications.

2. Relation between the α- and the JG β-relaxations

In the extended Coupling Model (CM), relaxation is initiated by the local primitive process. Due to intermolecular interaction the relaxation processes following the primitive relaxation are many-molecule in nature and dynamically heterogeneous. With the passage of time, the many-molecule relaxation evolves and ends up as the cooperative structural α-relaxation, which has the Kohlrausch–Williams–Watts (KWW) correlation function,

$$\phi(t) = \exp\left[-(t/\tau_\alpha)^{1-n}\right], \tag{1}$$

after averaging. Here τ_α is the α-relaxation time, $(1-n)$ is the Kohlrausch fractional exponent, and n is the coupling parameter. Since the primitive relaxation and the supposedly universal Johari–Goldstein (JG) secondary β-relaxation have similar properties and perform the same role as the precursor of the α-relaxation, their respective relaxation times τ_0 and τ_{JG} are approximately the same [17,24,25], *i.e.*,

$$\tau_0(T) \approx \tau_{JG}(T). \tag{2}$$

The familiar relation of the CM

$$\tau_\alpha = \left(t_c^{-n}\tau_0\right)^{1/(1-n)} \tag{3}$$

enables τ_0 to be calculated from the parameters τ_α and $(1-n)$ of the Kohlrausch correlation function of the α-relaxation time, and the crossover time t_c has the approximate value of 2×10^{-12} s for common polymeric and small molecular glass-formers [24,28]. On combining Eqs. (2) and (3), we have the relation,

$$\tau_\alpha \approx \left(t_c^{-n}\tau_{JG}\right)^{1/(1-n)}, \tag{4}$$

between τ_α and τ_{JG}. On the logarithmic scale, the relation is rewritten as

$$\log\tau_{JG} \approx (1-n)\log\tau_\alpha - 11.7n \tag{5}$$

from which τ_{JG} can be calculated from τ_α and n parameters of the α-relaxation. Good agreement between the calculated and the experimental values of τ_{JG} has been found repeatedly in many glass-forming substances including polymers [16,24–27]. Alternatively, Eq. (5) can be used to calculate n from the experimental τ_α and τ_{JG}. This method of deducing n or intermolecular cooperativity of the α-relaxation can be helpful in the P*n*AMAs because of the difficulty in obtaining it from the dispersion of the spectra. The strong overlap of the α-relaxation with the JG β-relaxation having sizeable relaxation strength creates large uncertainty in the value of n obtained by fitting the spectra. Throughout this paper, we are interested in the relation between the α- and the JG β-relaxation times when they are decoupled from each other. We do not consider the so-called αβ relaxation at higher temperatures where the α- and the JG β-relaxations merge together and can be considered practically as one process.

The β-relaxation in the P*n*AMAs originating from the ester side-group motion has previously been characterized by several multidimensional NMR experiments on atactic samples [6,17–22]. For the lower members, methyl and ethyl, it involves 180° flips of the planar ester side group around the C–C bond to the backbone and coupled with restricted rocking fluctuations of the backbone along its local extended chain axis. In one study it was reported that approximately 50% of the side groups undergo 180° flips coupled to approximately 25° rotations around the local chain axis [21]. The main-chain rocking motion in PEMA is ±17° at and below T_g, but its amplitude increases with increasing temperature and is ±50° at 30 K above T_g. Since the motion involves also the main chain, the β-relaxation of the P*n*AMAs is likely the JG β-relaxation according to the criteria laid down in Ref. [16] as the precursor of the local segmental α-relaxation. For poly(*n*-methyl methacrylates) (PMMA) dielectric measurement [29], and for PEMA dielectric relaxation and ^{13}C NMR measurements [18] have been reported in the literature which indicate that the Arrhenius temperature dependence of the JG β-relaxation times changes at a temperature close to T_g. Stronger temperature dependence is observed above T_g compared to the Arrhenius temperature dependence observed at temperatures significantly below T_g. This is one of the criteria for identifying a secondary relaxation to be the JG β-relaxation [16]. Hence, Eqs. (4) and (5) should be applicable to the P*n*AMAs. In the following section, we shall use these relations to interpret the collection of experimental data on the changes of dynamics with structural modifications.

3. Dependence of dynamics on structure

The chemical and physical structures of the P*n*AMAs can be changed in various ways. Accompanying the changes of structure are the changes of intermolecular coupling and cooperativity and consequently the α-relaxation dynamics. In this section we consider various changes of structure and show that the corresponding changes in dynamics can all be

consistently interpreted by the CM through the changing relation between τ_α and τ_{JG}.

3.1. Changing the number, C, of alkyl carbon atoms per side chain of PnAMA

The alkyl side chain like ethylene is much more mobile than the repeat units on the main chain. It is well known that the effect of the mobile side chains on the segmental α-relaxation is like a small molecule plasticizer. X-ray scattering and relaxation spectroscopy experiments have shown for higher P*n*AMAs that the alkyl groups of different monomeric units aggregate in the melt and form self-assembled alkyl nanodomains [6,7,30] with a typical size of 0.5–2 nm. The larger the number C of alkyl carbon atoms per side chain, larger is the volume fraction of the alkyl side chain and the size of the nanodomains, faster is the α-relaxation and lower is the glass transition temperature T_g. In the framework of the CM, the mobile alkyl nanodomains mitigate intermolecular coupling/constraints, decrease the coupling parameter of the α-relaxation, and it follows from Eq. (3) of the CM that the α-relaxation time τ_α is reduced. Thus, on increasing C and concomitantly the volume fraction of the alkyl nanodomains, the immediate effect is the further reduction of the intermolecular coupling and further increase of the mobility of the α-relaxation. A decrease in intermolecular coupling and a smaller coupling parameter n normally correspond to a narrower KWW dispersion given by Eq. (1). However, in the higher P*n*AMAs, there are concentration fluctuations due to spatial heterogeneity of nanophase separation, leading to a distribution of n's. This effect and the overlap with the nearby JG relaxation mean that any of the distributed n's cannot be deduced by fitting the time or frequency dependence of the spectrum by Eq. (1), and the expected decrease of intermolecular coupling with increasing length of the side chain cannot be verified. Nevertheless, coming to the rescue is Eq. (5), from which the most probable value of n in the distribution can be deduced from the experimental values of τ_α and τ_{JG} and the equation,

$$n = \frac{\log \tau_\alpha(T) - \log \tau_{JG}(T)}{11.7 + \log \tau_\alpha(T)} \tag{6}$$

An objective comparison of the most probable value of n of the P*n*AMAs is at the same τ_α. One choice is $\tau_\alpha = 100$ s, which is often used in dielectric relaxation measurements to define T_g. With this choice, $n(T_g)$ is given by $[\log \tau_\alpha(T_g) - \log \tau_{JG}(T_g)]/13.7$. Comprehensive data of τ_α and τ_{JG} have been collected for the amorphous high molecular weight poly(alkyl methacrylate)s from methyl ($C = 1$) to lauryl ($C = 12$) as shown in Fig. 5 of Ref. [7]. The Arrhenius plot of τ_α and τ_{JG} in this figure shows clearly with increasing C that $[\log \tau_\alpha - \log \tau_{JG}]$ decreases monotonically: PMMA (≈7 decades), PEMA (≈5.5 decades), poly(*n*-propyl methacrylates) (P*n*PrMA) (≈3.7 decades), poly(*n*-butyl methacrylates) (P*n*BMA) (≈3.3 decades) and P*n*HMA (≈3 decades). Hence from the relation, $n(T_g) = [\log \tau_\alpha(T_g) - \log \tau_{JG}(T_g)]/13.7$, the dielectric relaxation coupling parameter n at T_g is 0.51 for atactic PMMA, 0.40 for PEMA, 0.27 for P*n*BMA and 0.22 for P*n*HMA.

The steepness or "cooperativity" index or "fragility" defined by [31,32]

$$m = \mathrm{d}(\log \tau_\alpha)/\mathrm{d}\left(T_{ref}/T\right), \tag{7}$$

where the reference temperature T_{ref} is the temperature at which $\tau_\alpha(T_{ref})$ attains an arbitrarily chosen long time such as 100 s, is another quantity that has been obtained for the P*n*AMAs. It has been shown that m decreases with increasing C [33–35]. Hence, this trend together with the empirically established correlation [31,32] between n and m (*i.e.*, the quantity m increases in parallel with n when restricted to glass-formers in the same family) provides another support for decrease of n with increasing C.

3.2. Change in tacticity

Structure of PMMA or PEMA can be varied by preparing samples with different tacticity. Syndiotactic and atactic PMMA and PEMA have higher T_g than the isotactic homologues, i-PMMA and i-PEMA, respectively, which suggests the possibility that the coupling parameters of the isotactic homologues are smaller. This is because according to Eq. (4) smaller n leads to shorter τ_α for the same τ_0. Confirmation of i-PMMA having smaller n than its corresponding syndiotactic and atactic homologues is provided by Eq. (5) by comparing $\log \tau_\alpha - \log \tau_{JG}$ at $\tau_\alpha = 100$ s of bulk i-PMMA obtained by Hartmann et al. [8] with that of an atactic high molecular weight PMMA [7]. The comparison is made for PMMA in Fig. 1, where the star symbols indicate τ_α and τ_{JG} of bulk i-PMMA and squares are for the syndiotactic PMMA. The rest of the data in Fig. 1 are for thin films of i-PMMA, which will be discussed in another subsection. Fig. 1 shows that at

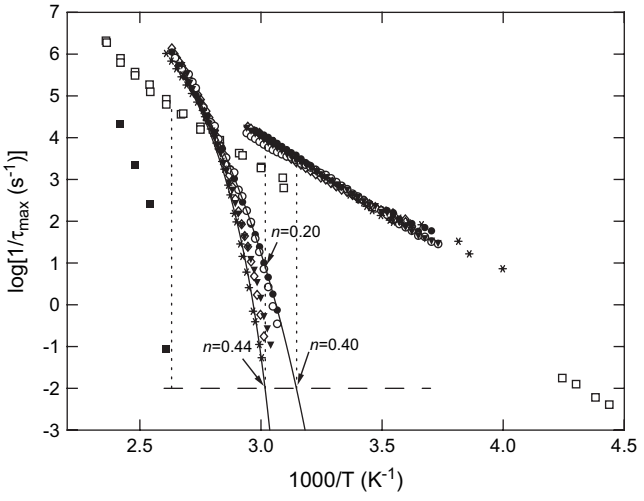

Fig. 1. Relaxation map of bulk s-PMMA (data from Ref. [1]) and i-PMMA and thin films of isotactic PMMA with $M_w = 164.7$ kg/mol (data from Ref. [2]). Closed squares: τ_α of bulk s-PMMA; open squares: τ_{JG} of bulk s-PMMA; stars: τ_α and τ_{JG} of bulk i-PMMA. Open diamonds, filled inverted triangles, open circles and closed circles are τ_α and τ_{JG} of i-PMMA films with thickness equal to 137, 68, 36 and 20 nm, respectively.

the glass transition temperatures T_g of the two homologues defined by $\tau_\alpha(T_g) = 100$ s, the separation between the α- and the JG β-relaxations measured by $\log \tau_\alpha(T_g) - \log \tau_{JG}(T_g)$ of the syndiotactic PMMA is larger than that of i-PMMA by about one decade. Thus, via Eq. (6), syndiotactic or atactic PMMA has larger n (=0.51) than i-PMMA ($n = 0.44$). It can be seen by inspection of Fig. 1 that the larger $\log \tau_\alpha(T_g) - \log \tau_{JG}(T_g)$ of syndiotactic or atactic PMMA than i-PMMA necessarily implies that the former has a higher T_g than the latter. Equivalently, we can say that larger intermolecular coupling or n is responsible for the higher T_g of syndiotactic or atactic PMMA than i-PMMA.

Empirically, n correlates with m [31,32]. In Fig. 2, we compare the T_g-scaled temperature dependence of τ_α of i-PMMA with that of syndiotactic (85%) PMMA [29]. Shown are the T_g-scaled Vogel–Fulcher–Tammann–Hesse fits to τ_α of these two polymers, with T_g defined by $\tau_\alpha(T_g) = 100$ s. Indeed, the steepness index m of the syndiotactic PMMA is 181 and larger than 147 of i-PMMA, in accord with the correlation.

By inspection of Fig. 1, it can be seen that the JG relaxation time is nearly the same at temperatures where both i-PMMA and ordinary PMMA are in the glassy state. This is perhaps not surprising when considering the fact that the JG relaxation is local and hence not sensitive to tacticity or the details of the arrangements of the side groups from one repeat unit to another. The same is true on comparing τ_{JG} of i-PEMA with that of atactic PEMA as found by the CODEX NMR experiment [6]. In fact, τ_{JG} of i-PEMA coincides with that of atactic PEMA at temperatures where both are in the glassy state. Another indication of the insensitivity of τ_{JG} to tacticity is the dielectric data of two PEMA samples with different tacticity and molecular weights [7]. The data of τ_{JG} and τ_α are reproduced in an Arrhenius plot in Fig. 3. The closed diamonds represent the data of the sample with 88% syndiotactic diads, $M_n = 4.9$ kg/mol and $M_w/M_n = 1.07$, and open squares are for the other sample with 78% syndiotactic diads,

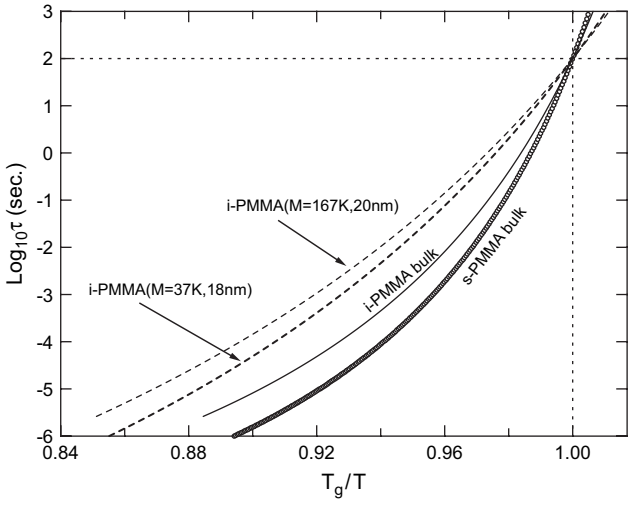

Fig. 2. Cooperativity plot of the Vogel–Fulcher–Tammann–Hesse fits of $\log \tau_\alpha$ against T_g/T of bulk s-PMMA, bulk i-PMMA, and 20 nm thin film of i-PMMA with $M_w = 167$ kg/mol, and 18 nm thin film of i-PMMA with $M_w = 37$ kg/mol.

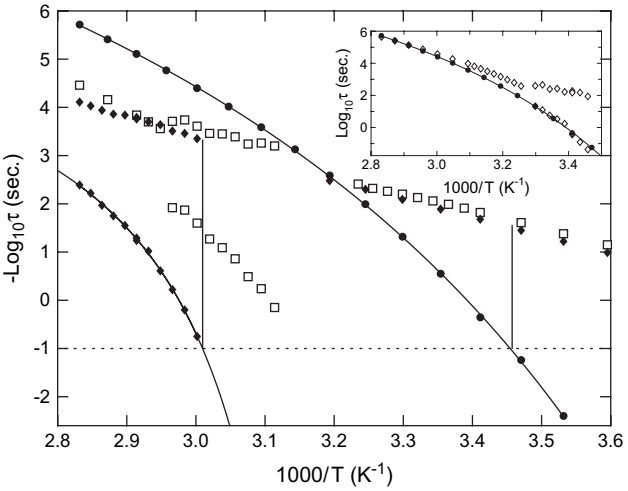

Fig. 3. Arrhenius plot of τ_α and τ_{JG} for three PEMA samples with different molar weights and tacticity. Closed diamonds: 88% syndiotactic diads, $M_n = 4.9$ kg/mol, $M_w/M_n = 1.07$ (S. Reissig, Ph.D. thesis, Universität Halle, 1999). Open squares: 78% syndiotactic diads, $M_n = 7.1$ kg/mol, $M_w/M_n = 1.37$ (S. Reissig, Ph.D. thesis, Universität Halle, 1999). Closed circles: 92% isotactic triads, $M_w = 47.2$ kg/mol and $M_w/M_n = 1.17$. Shown in the inset are τ_α of a low molecular weight PEMA ($M_w = 1.6$ kg/mol) with 80% syndio diads (open diamonds) and the τ_α of i-PEMA with $M_w = 47.2$ kg/mol and 92% isotactic triads (closed circles). They are nearly the same. Shown also is the τ_{JG} of the former (open diamonds).

$M_n = 7.1$ kg/mol and $M_w/M_n = 1.37$. Fig. 3 shows that the sample with lesser syndiotactic diads (78%) has a shorter τ_α (open squares) at the same temperature and hence a lower T_g, but its τ_{JG} (also open squares) is the same as that (also closed diamonds) of the sample with more syndiotactic diads (88%). Broadband dielectric measurements of i-PEMA have not been reported before. Therefore measurements on a high molecular weight i-PMMA ($M_w = 47.2$ kg/mol and $M_w/M_n = 1.17$) have been performed. The sample was kindly provided by Dr. M. Gaborieau (MPI-P Mainz) and is from the same source as that used in recent NMR studies [6]. It has high isotacticity with 92% isotactic triads. The isothermal dielectric loss spectra obtained for a number of temperatures are presented in Fig. 4. Data taken at higher temperatures are not shown for the sake of clarity. From the angular frequencies at the loss peaks, ω_{max}, we obtain directly τ_α as the reciprocals of ω_{max}. No fit to any empirical function including the Fourier transform of the Kohlrausch function is attempted to determine τ_α for the reason which will become clear later. Shown in the Arrhenius plot of Fig. 3 are τ_α of i-PMMA (closed circles), and the line drawn through them is the fit by the Vogel–Fulcher–Tammann–Hesse equation, $\log \tau_\alpha = [-12.94 + 958.9/(T - 220.69)]$.

Before we discuss the spectra in Fig. 4, let us return to Fig. 3 and consider the changing relation between τ_α and τ_{JG} with change in tacticity at $\tau_\alpha = 10$ s. We make use of the fact established by CODEX NMR [6] that τ_{JG} of i-PEMA coincides with that of atactic PEMA. Then the lengths of the vertical lines in Fig. 3 indicate the size of $\log \tau_\alpha - \log \tau_{JG}$ for the two homologues when $\tau_\alpha = 10$ s. We have chosen $\tau_\alpha = 10$ s because the measured τ_α of the 88% syndiotactic PEMA does not go beyond 10 s. The same conclusion is

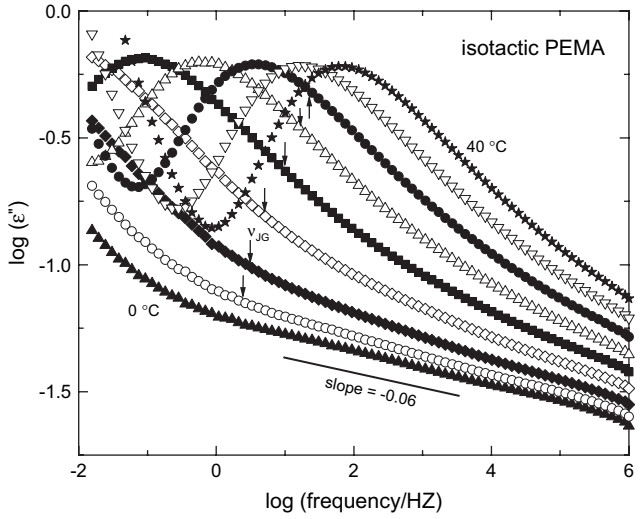

Fig. 4. Isothermal dielectric loss spectra of PEMA with 92% isotactic triads, and $M_w = 47.2$ kg/mol ($M_w/M_n = 1.17$). From left to right, the temperatures are 0, 5, 10, 15, 20, 25, 30, 35, and 40 °C. The location of each vertical arrow indicates the JG relaxation frequency. For further explanation, see text.

reached if we chose $\tau_\alpha = 100$ s and use the Vogel–Fulcher–Tammann–Hesse fit (shown as line in Fig. 3) to obtain its value. Clearly, $\log \tau_\alpha - \log \tau_{JG}$ is significantly smaller for i-PEMA than the 88% syndiotactic PEMA. In other words, the JG relaxation is located closer to the α-relaxation in i-PEMA than in the 88% syndiotactic PEMA. From Eq. (6), we deduce $n = 0.34$ for the 88% syndiotactic PEMA and $n = 0.21$ for the i-PEMA when $\tau_\alpha = 10$ s. At $\tau_\alpha = 100$ s, we have $n = 0.40$ for the syndiotactic PEMA and $n = 0.25$ for i-PEMA. Like PMMA discussed earlier, the larger intermolecular coupling or n of syndiotactic PEMA than that of i-PMMA is responsible at least in part for the higher T_g of the former than the latter.

The relaxation map given by Fig. 3 enables us to predict τ_{JG} that corresponds to τ_α, for each temperature the isothermal dielectric spectrum of i-PEMA shown in Fig. 4 was taken. The location of the frequency ν_{JG} corresponding to τ_{JG}, *i.e.*, $\nu_{JG} \equiv (1/2\pi\tau_{JG})$, is indicated by the vertical arrow in Fig. 4, pointing at the loss data for each temperature. The α-peak frequency ν_α is not much lower than ν_{JG}, suggesting significant overlap of the contribution to the dielectric loss by the α- and the JG β-relaxations. Consequently, due to the overlap, not only the JG β-relaxation cannot be resolved but also the α-peak is broaden considerably than that given by the Kohlrausch function (Eq. (1)) with n deduced in the above from $\log \tau_\alpha - \log \tau_{JG}$ and Eq. (6). We make no attempt to deconvolute the α- and the JG β-relaxations by any commonly used procedure because the two are too close to each other, and the dielectric strength of the JG β-relaxation is not small compared with that of the α-relaxation. Small molecule glass-formers such as propylene carbonate and glycerol [16,24] have small coupling parameter n like i-PEMA. Again, the proximity of ν_α to ν_{JG} renders the JG relaxation unresolved. However, unlike i-PEMA, the relaxation strength of the unresolved JG relaxation in these small molecule glass-formers is much smaller, and its contribution appears as an excess wing at the high frequency flank of the α-loss peak. As a result, the α-loss peak is not significantly broadened and its coupling parameter can be obtained by fitting it to the Fourier transform of the Kohlrausch function. The experimental fact that the dielectric strength of the JG relaxation, $\Delta\varepsilon_\beta$, of i-PEMA is not small compared with $\Delta\varepsilon_\alpha$ of the α-relaxation is not surprising if one recalls that in high molecular weight syndiotactic PEMA the height of the resolved JG loss peak is even greater than that of the α-relaxation (see for example the loss data of 150 kg/mol of PEMA (78% syndiotactic diads) in Fig. 17 of Ref. [7]).

A new feature emerges in the loss spectra at lower temperatures and higher frequencies. The feature is the nearly constant loss (NCL), coming from some relaxation process that precedes the JG relaxation in time. The weak frequency dependence of the NCL is made evident by comparing with the line drawn with slope −0.06 in the plot of $\log \varepsilon''$ against $\log \nu$ (Fig. 4). The NCL is a universal feature of glass-forming substances [24,25] and other cooperatively relaxing systems such as ion conductivity relaxation in molten, glassy and even crystalline ionic conductors [36]. The NCL has been suggested to originate from fluctuations of cages at times when molecules are caged. The NCL terminates at times marking the onset of the local JG relaxation (or equivalently the primitive relaxation of the CM) because it causes cages to decay. Thus, τ_{JG} and τ_0 are the upper bounds (in order of magnitude) of the NCL time regime, and equivalently the corresponding frequencies ν_{JG} and ν_0 are the lower bounds of the NCL frequency regime. This relation has been verified in a number of glass-formers and ionic conductors, where the NCL is observed and ν_{JG} and ν_0 can be determined. It holds also for i-PEMA as can be seen in Fig. 4 that ν_{JG} or ν_0 is indeed the upper bound (order of magnitude) of the NCL frequency regime.

3.3. Change by nanoconfinement

When a high molecular weight polymer is cast in a thin film with thickness of nanometers, there are effects that can change the dynamics of α-relaxation. Assuming there is no chemical bonding or physical interaction of the surface molecules with outside, motion of molecules at the surface is no longer constrained by other molecules on one side and lesser many-molecule dynamics are involved. If the thickness h is smaller than twice the radius of gyration, the confined chains become more orientated and this effect also contribute to higher mobility. In the CM description [37] of the α-relaxation, the coupling parameter n_1 of this surface layer molecules is significantly reduced from the bulk value n_b. Their correlation function is still the Kohlrausch function, $\phi_1(t) = \exp[-(t/\tau_{\alpha 1})^{1-n_1}]$, where the relaxation time $\tau_{\alpha 1}$ is given by $\tau_{\alpha 1} = [t_c^{-n_1}\tau_0]^{1/(1-n_1)}$, the analogue of Eq. (3), with $n_1 < n_b$. The coupling parameter n_2 for molecules in the second layer is also reduced from n_b because of proximity to the more mobile first layer, but the reduction is lesser and hence $n_1 < n_2 < n_b$. The correlation function of molecules in the second layer is again the Kohlrausch

function, $\phi_2(t) = \exp[-(t/\tau_{\alpha 2})^{1-n_2}]$, and the relaxation time $\tau_{\alpha 2}$ is given by $\tau_{\alpha 2} = [t_c^{-n_2}\tau_0]^{1/(1-n_2)}$. Eq. (3) indicates that τ_α is a monotonic increasing function of n. From $n_1 < n_b$ and $n_1 < n_2$, we have $\tau_{\alpha 1} < \tau_b$ and $\tau_{\alpha 1} < \tau_{\alpha 2}$ provided $\tau_0 \ll t_c$, which is well satisfied in experiments of long time scales. Seeing not as mobile molecules on the surface side than the second layer, the third layer molecules have coupling parameter n_3 larger than n_2, and $\tau_{\alpha 3}$ longer than $\tau_{\alpha 2}$. Repeating the argument onto the j-th layer, we have $n_1 < n_2 < n_3 < \ldots < n_j < n_b$, $\tau_{\alpha j} = [t_c^{-n_j}\tau_0]^{1/(1-n_j)}$, and $\tau_{\alpha 1} < \tau_{\alpha 2} < \tau_{\alpha 3} < \ldots < \tau_{\alpha j} < \tau_{\alpha b}$. What we have is a smooth change in the cooperative many-molecule dynamics across the film. For a thick enough film, eventually at some depth the bulk dynamics with parameters n_b and $\tau_{\alpha b}$ are recovered. Relaxation in thin i-PMMA films has been studied by dielectric spectroscopy [8], where the aluminum electrodes are not supposed to have chemical and physical interactions with the i-PMMA. The α- and JG β-relaxations of the i-PMMA thin films measured come from the contributions of all layers. Their relaxation times shown in Fig. 2 are some average of $\{n_j\}$, with values n_{avg} less than n_b. Thinner film has smaller n_{avg}. The expected results, $n_{avg} < n_b$ and monotonic decrease of n_{avg} with i-PMMA film thickness, are supported by the observed concomitant decrease of $\log \tau_\alpha(T_g) - \log \tau_{JG}(T_g)$ as shown in Fig. 1. By Eq. (6), the 18 nm thin i-PMMA has $n_{avg}(T_g) = 0.40$, smaller than $n = 0.44$ of bulk i-PMMA.

From Fig. 1, it can be seen that smaller n_{avg} of the thin film compared with n_b of bulk is accompanied by a weaker T_g-scaled temperature dependence of τ_α and correspondingly smaller m. Bulk i-PMMA has $m = 147$, while the 18 nm film of 37,000 molecular weight i-PMMA has $m = 93$, and the 20 nm film of 167,000 molecular weight i-PMMA has $m = 84$. For the same thin film thickness, high molecular weight polymer has more induced orientations due to confinement, and hence smaller $\log \tau_\alpha(T_g) - \log \tau_{JG}(T_g)$ and n_{avg}, as found. The steepness index m is correspondingly smaller for the higher molecular weight i-PMMA (see Fig. 2). Although the change is not large, 84 *versus* 93, the change is in accord with the empirical correlation between n and m.

An opposite effect on intermolecular coupling and n is obtained when the i-PMMA thin film ($T_g \approx 56$ °C) is sandwiched between thin layers of the incompatible polystyrene polymer with higher $T_g \approx 97$ °C as studied by Wübbenhorst et al. using dielectric spectroscopy [38]. The difference from the previous case is that there are intermolecular interactions between the i-PMMA molecules and the less mobile polystyrene molecules confining them. The interfaces between the central i-PMMA film and the PS films are not sharp but are the i-PMMA-PS interdiffusion layers with thickness of 4–5 nm. Nevertheless, the i-PMMA segments in the interdiffusion layers, due to the presence of the less mobile PS, are intermolecularly more constrained and have larger coupling parameters n, and the effects propagate layer by layer into the i-PMMA film. The situation is essentially the same as that of a Lennard–Jones (LJ) liquid thin film confined on both sides by frozen binary LJ liquids [39]. The expected increase of n of the LJ layers and the attenuation of the effect into the center of the film, *i.e.*, $n_1 > n_2 > n_3 > \ldots > n_j > \ldots > n_b$, $\tau_{\alpha j} = [t_c^{-n_j}\tau_0]^{1/(1-n_j)}$, and $\tau_{\alpha 1} > \tau_{\alpha 2} > \tau_{\alpha 3} > \ldots > \tau_{\alpha j} > \ldots > \tau_{\alpha b}$. This CM description [37] is in accord with the results found by molecular dynamics simulation [39]. The same description applies to the i-PMMA thin film confined between two PS thick films. Since dielectric spectroscopy was used in the experiment, Wübbenhorst et al. can only observe an averaged T_g of the i-PMMA film. The averaged T_g of the i-PMMA film was observed to be higher than that of bulk i-PMMA as predicted. The increase of T_g is larger for thinner i-PMMA films as expected. As has been discussed before, the relaxation time of the local JG β-relaxation of the sandwiched i-PMMA thin film is the same as given by the continuation of the Arrhenius dependence shown in Fig. 1 to higher temperature than T_g of bulk i-PMMA. Then, naturally $\log \tau_\alpha(T_g) - \log \tau_{JG}(T_g)$ of the sandwiched i-PMMA film increases with decreasing film thickness and, via Eq. (6), this is another indication of the increase in n_{avg}.

3.4. Change with molecular weight

Decreasing the molecular weight of a polymer below its entanglement molecular weight usually is accompanied by a decrease in T_g. The change is due to the increasing concentration of chain ends which, having higher mobility than the inner bonded repeat units, acts like a plasticizer. In the CM, the presence of a more mobile component B reduces the coupling parameter n of the other component A. Thus, a sample with lower molecular weight will have a smaller value of n. However, in any mixture there are concentration fluctuations of the two components, giving rise to a distribution of n's. The distribution causes additional broadening of the frequency dispersion of the α-relaxation of component A beyond that given by the Kohlrausch function (Eq. (1)) if n is taken to be any one in the distribution. The presence of this excess broadening has been shown in low molecular weight polystyrene by a combination of photon correlation spectroscopy and creep compliance measurement [40]. None of the n's in the distribution can be deduced from the observed dispersion and hence the expected decrease of the n's with decreasing molecular weight cannot be verified directly. The P*n*AMAs offer a way to test this prediction by examining the change of $\log \tau_\alpha(T_g) - \log \tau_{JG}(T_g)$ with decreasing molecular weight. The Arrhenius plot of τ_α and τ_{JG} of four PEMA samples obtained by Reissig et al. [41] is shown in Fig. 5. The samples all have nearly the same 78% of syndio diads but different number average molecular weights of 150, 21, 7.1 and 1.6 kg/mol with the calorimetric T_gs equal to 74, 55, 42 and 10 °C, respectively. Since now we are working with the dielectric relaxation data in Fig. 5 where the measured dielectric α-relaxation times τ_α are not longer than 10 s, for all samples the reference temperature T_{10} is defined as the temperature at which τ_α is equal to 10 s, *i.e.*, $\tau_\alpha(T_{10}) = 10$ s. The three thick vertical lines in Fig. 5 are drawn to indicate the magnitudes of $\log \tau_\alpha(T_{10}) - \log \tau_{JG}(T_{10})$ for three PEMAs with molecular weights of 150, 7.1 and 1.6 kg/mol. The data of the 21 kg/mol sample are not treated in the same manner because its τ_α had not

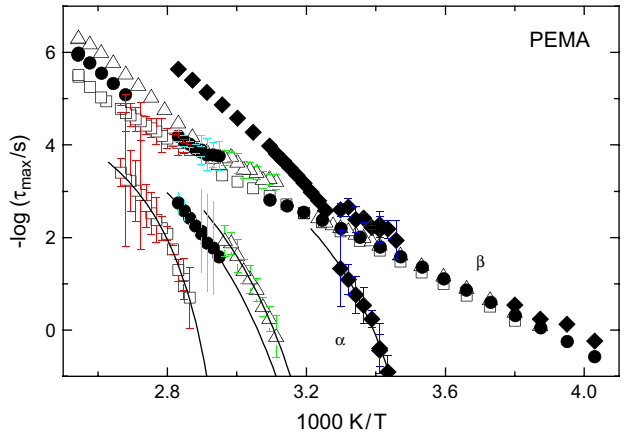

Fig. 5. Arrhenius plot for PEMA samples with different molar weights (open squares, 150 kg/mol; closed circles, 21 kg/mol; open triangles, 7.1 kg/mol; closed diamonds, 1.6 kg/mol). Data are reproduced from Ref. [41] with permission.

been measured for sufficiently long times. It is clear that $\log \tau_\alpha(T_{10}) - \log \tau_{JG}(T_{10})$ decreases with decreasing molecular weight, and the coupling parameters $n(T_{10})$ deduced from Eq. (6) are 0.37, 0.31 and 0.24 for PEMAs with molecular weights of 150, 7.1 and 1.6 kg/mol, respectively.

The τ_α of the low molecular weight PEMA ($M_w = 1.6$ kg/mol) with 80% syndio diads are nearly the same as the τ_α of i-PEMA with $M_w = 47.2$ kg/mol and 92% isotactic triads as shown in the inset of Fig. 3. Shown also is the τ_{JG} of the former, which can be assumed to be the same as τ_{JG} of the latter. This follows from the CODEX NMR results [6] that τ_{JG} of i-PEMA and high molecular weight syndiotactic PEMA are the same, and the fact that τ_{JG} of syndiotactic PEMA is independent of molecular weight (see Fig. 5). The indication is that τ_α and τ_{JG} are the same either by lowering the molecular weight of syndiotactic PEMA to 1.6 kg/mol or by changing tacticity to 92% isotactic triads. The *n*-butyl methacrylates ranging from the monomer to the high molecular weight polymers have been recently studied [42]. From this study, it becomes clear that differences in other parameters such as calorimetric or dielectric relaxation strength do exist although the traces in the Arrhenius plot are identical.

3.5. Change by copolymerization

Serious chemical modification of a poly(*n*-alkyl methacrylate) can be achieved by random copolymerization with a monomer such as styrene having a completely different molecular structure. Polystyrene has a significantly higher T_g than P*n*BMA, which implies that the styrene monomers have lower mobility than *n*BMA monomers. Therefore the coupling parameter *n* of the α-relaxation originating from the *n*BMA monomers will increase with increasing styrene content in the random copolymer. Dielectric relaxation measurements have been made on a series of poly(*n*-butyl methacrylate-*stat*-styrene) copolymers with styrene contents ranging from 0 to 66 mol% utilizing the dielectric relaxation data of Kahle et al. [43]. Since styrene has negligible dipole moment compared with *n*BMA, the dielectric data reflect the motion of the *n*BMA monomers including the α- and the JG β-relaxations that originate from them. The α-relaxation time τ_α is shifted to longer times consistent with the increase of the coupling parameter *n* of the *n*BMA. At sufficient high styrene mole fraction of 38% and beyond, the τ_{JG} of the *n*BMA is changed as well. The combined changes of τ_α and τ_{JG} result in a monotonic increase of the separation, $[\log \tau_\alpha(T_g) - \log \tau_{JG}(T_g)]$, when the styrene mole fraction is increased up to 66% [44]. This trend implies that *n* indeed increases with styrene content according to Eq. (6). Another support of this conclusion is the concomitant increase of the steepness or the 'fragility' index *m* [44].

3.6. Change by crosslinking

Chemical crosslinks when introduced enhance intermolecular constraints and hence the coupling parameter *n*. It was reported that, on crosslinking PMMA, τ_{JG} does not change, which has been rationalized as due to the local nature of the JG β-relaxation [45]. On the other hand, τ_α increases significantly with the density of crosslinks. Hence $\log \tau_\alpha(T_g) - \log \tau_{JG}(T_g)$ increases with crosslink density and this lend support to the expected increase of *n*, again by Eq. (6). Further support comes from the increase of the steepness index *m* and the width of the dispersion of the α-relaxation obtained by dynamic mechanical relaxation and creep compliance measurements [45].

3.7. Change in the isomers of poly(butyl methacrylate)

Poly(isobutyl methacrylate) (P*i*BMA), poly(*tert*-butyl methacrylate) (P*t*BMA), and poly(*n*-butyl methacrylate) (P*n*BMA) are three isomers of poly(butyl methacrylate). P*i*BMA and P*t*BMA are related to P*n*BMA by replacing the *n*-alkyl group with *iso*- and the *tert*- alkyl groups, respectively. The glass transition temperatures from DSC are 298, 338 and 363 K for P*n*BMA, P*i*BMA and P*t*BMA, respectively [46]. The dynamics in these three poly(butyl methacrylate) isomers were studied by dielectric and mechanical spectroscopies [46]. The data show the presence of the α-relaxation, the JG β-relaxation and two additional secondary relaxations at high frequencies. Although the α-relaxation time τ_α is altered significantly following the change of T_g, the secondary relaxation times including τ_{JG} have almost the same Arrhenius temperature dependence in the glassy state of the three isomers, consistent with the fact that they are the local relaxations unaffected by intermolecular coupling. The increasingly shorter and more rigid side groups in the order of P*n*BMA, P*i*BMA and P*t*BMA have the effects of reducing the internal plasticization and increasing the steric hindrance, and hence intermolecular coupling of the cooperative α-relaxation. This expectation is supported by the increase of $\log \tau_\alpha(T_g) - \log \tau_{JG}(T_g)$ in going from P*n*BMA to P*i*BMA and to P*t*BMA and Eq. (6). As can be seen by inspection of Fig. 6 in Ref. [46], $\log \tau_\alpha(T_g) - \log \tau_{JG}(T_g)$ increases in the order of P*n*BMA, P*i*BMA and P*t*BMA, and thus, according to Eq. (6),

the coupling parameter n increases. At a temperature near T_g of P*i*BMA (see Fig. 6b of Ref. [46], where τ_α ($\approx 10^{4.2}$ s) and τ_{JG} ($\approx 10^{-2}$ s)), we deduce by Eq. (6) the value $n = 0.39$ for P*i*BMA. This is not too different from the range of values $n = 0.41-0.45$ of the 520 nm thick film near T_g from the second-order macroscopic susceptibility, $\chi^{(2)}(t)$, measurement of Torkelson et al. [47]. On the other hand, at a temperature near T_g of P*t*BMA (see Fig. 6c of Ref. [46]), where τ_α ($\approx 10^{4.2}$ s) and τ_{JG} ($\approx 10^{-3.8}$ s), we deduce by Eq. (6) the value $n = 0.53$ for P*t*BMA. The increase of intermolecular coupling and the coupling parameter deduced from the corresponding increase of $\log \tau_\alpha(T_g) - \log \tau_{JG}(T_g)$ is additionally supported by the increase of the steepness index $m(T_g)$ from 44.7 for P*n*BMA to 67.3 for P*i*BMA, and to 128 for P*t*BMA.

4. Discussion and conclusion

The Johari–Goldstein (JG) secondary relaxation as a precursor of the many-molecule relaxation that culminates at the cooperative primary α-relaxation need to be considered in order to have a more complete description of the molecular dynamics of glass-forming substances. The fundamental nature of the JG relaxation and the possible role it plays are suggested by its many general properties which mimic that of the α-relaxation [16,48,49]. One remarkable property is the strong correlation at constant τ_α between the ratio τ_α/τ_{JG} (or $\log \tau_\alpha - \log \tau_{JG}$) and the coupling parameter n of the Coupling Model (CM). For neat glass-formers without microscopic heterogeneities such as crosslinks or nanophase separated domains in higher members of the poly(*n*-alkyl methacrylates), the coupling parameter n is exactly that appearing as the fractional exponent $(1 - n)$ of the Kohlrausch correlation function for the α-relaxation. This correlation predicted by the CM has been well established over the recent past for many glass-formers of various types [16,24–27]. The coupling parameter n governs τ_α and its properties. An example is given by the recent experimental findings of the invariance of the dispersion (*i.e.*, n) on changing the combinations of pressure and temperature while maintaining τ_α constant [50]. The stretching of the α-dispersion beyond that given by the Debye relaxation is also governed by n, indicating that n is a measure of the extent of the cooperative many-molecule dynamics. Hence, n increases with intermolecular interaction and constraints, and naturally it depends on the chemical and physical structures of the glass-former. There are many different variations of the structure of the poly(alkyl methacrylate)s, and the variations offer excellent opportunities for examining how structure determines n and the molecular dynamics. The effort is enhanced by the ever presence of the JG β-relaxation in all variations, which allows us to determine $\log \tau_\alpha - \log \tau_{JG}$ and use the relation given by Eq. (6) to deduce the coupling parameter n. The results are in accord with the expected increase of n with increase of intermolecular interaction and constraints, although in many cases n cannot be directly obtained from the measured frequency dispersion of the α-relaxation due to broadening by various sources of heterogeneity. Additional support comes from the observed changes of m with changes in structure and the empirical correlation between n and the steepness or the 'fragility' index m, which also follows from the CM. In some special cases, n can be determined directly by fitting the Kohlrausch function to the observed α-relaxation. Only in these special cases that all parameters, n, τ_α, and τ_{JG}, are known from experiment to test Eq. (6), and the results are in quantitative agreement with the CM prediction.

As seen from the results presented, the JG relaxation time τ_{JG} is insensitive to change of tacticity, molecular weight, nanoconfinement, and crosslinking, a behavior consistent with the local nature of the JG relaxation. For PEMA, the same Arrhenius equation applies to describe the temperature dependence of τ_{JG} in the glassy state of PEMA of different tacticity (Fig. 3) and molecular weights (Fig. 5). This fact together with Eq. (5) suggests that the change of T_g of PEMA with tacticity and molecular weight is caused principally by the corresponding change in intermolecular coupling or n. From PMMA ($C = 1$) up to P*n*PeMA ($C = 5$), the τ_{JG}'s of these P(*n*AMA)s in the glassy states also are well described by similar and approximately the same Arrhenius temperature dependences (see Fig. 5 in Ref. [7]). Again, this behavior of τ_{JG}'s of PMMA ($C = 1$) up to P*n*PeMA ($C = 5$) suggests that the variations of the T_g's of these polymers are principally determined by their different n's.

Before closing, we mention a similar scenario of change of relaxation in the self-assembled alkyl nanodomains formed by nanophase separation of incompatible main and side chain parts in higher P*n*AMA. The size of the alkyl nanodomains increases with the number of carbon atoms, C, in the side chain, ranging from 0.5 to 1.5 nm when C is increased from 4 to 10 [30]. A polyethylene-like glass transition α_{PE} occurs within the alkyl nanodomains. The dielectric, mechanical and calorimetric relaxation data suggest that an unresolved Johari–Goldstein secondary relaxation (β_{PE}) is present in addition to the primary α_{PE}-relaxation of this polyethylene-like glass transition [26]. Since polyethylene has the simplest chemical structure among carbon backbone polymers, the α_{PE}-relaxation of the alkyl nanodomains has weak intermolecular coupling and small n. The ratio τ_α/τ_{JG} of the relaxation times of the two processes (or the separation distance, $\log \tau_\alpha - \log \tau_{JG}$) is consistent with the weakly cooperative nature of the α_{PE}-relaxation, which is corroborated by its low steepness or 'fragility' index [26,30,51].

Acknowledgements

The authors thank Dr. Marianne Gaborieau (MPI-P Mainz) for kindly providing the i-PEMA sample used in this study. The work performed at the Naval Research Laboratory was supported by the Office of Naval Research.

References

[1] Pakula Tadeusz. Macromol Symp 2004;214:307.
[2] Denizli BK, Lutz JF, Okrasa L, Pakula T, Guner A, Matyjaszewski K. J Polym Sci Part A Polym Chem 2005;43:3440.

[3] Rathgeber S, Pakula T, Urban V. J Chem Phys 2004;121:3840.
[4] Polanowski P, Pakula T. J Chem Phys 2002;117:4022.
[5] Shinoda H, Matyjaszewski K, Okrasa L, Mierzwa M, Pakula T. Macromolecules 2003;36:4772.
[6] Wind M, Graf R, Renker S, Spiess HW. Macromol Chem Phys 2005; 206:142.
[7] For references to works in the past and a review of various experiments, see: Beiner M Macromol Rapid Commun 2001;22:869.
[8] Hartmann L, Gorbatschow W, Hauwede J, Kremer F. Eur Phys J E 2002; 8:145.
[9] Ishida Y, Yamafuji K. Kolloid Z 1961;177:97.
[10] Heijboer J. Int J Polym Mater 1977;6:11.
[11] Laupretre F, Virlet J, Boyle JP. Macromolecules 1985;18:1846.
[12] Ribes-Greus Amparo, Gomez-Ribelles Jose L, Diaz-Calleja Ricardo. Polymer 1985;26:1849; Murthy SSN, Shahin Md. Eur Polym J 2006; 42:715.
[13] Fytas G. Macromolecules 1989;22:211.
[14] Johari GP, Goldstein M. J Chem Phys 1970;53:2372; Johari GP, Goldstein M. J Chem Phys 1971;55:4245.
[15] Johari GP. Ann NY Acad Sci 1976;279:117; J Non-Cryst Solids 2002; 307–310:317.
[16] Ngai KL, Paluch M. J Chem Phys 2004;120:857.
[17] Schmidt-Rohr K, Kudlik AS, Beckham HW, Ohlemacher A, Pawelzik U, Boeffel C, et al. Macromolecules 1994;27:4733.
[18] Kudlik AS, Beckham HW, Schmidt-Rohr K, Radloff D, Pawelzik U, Boeffel C, et al. Macromolecules 1994;27:4746.
[19] Kuebler SC, Schaefer DJ, Pawelzik U, Boeffel C, Spiess HW. Macromolecules 1997;30:6597.
[20] Domberger W, Reichert D, Garwe F, Schneider H, Donth E. J Phys Condens Matter 1995;7:7419.
[21] deAzevedo ER, Hu W-G, Bonagamba TJ, Schmidt-Rohr K. J Am Chem Soc 1999;121:8411.
[22] Wind M, Brombacher L, Heuer A, Graf R, Spiess HW. Solid State Nucl Magn Reson 2005;27:132.
[23] Ngai KL, Tsang KY. Phys Rev E 1999;60:4511.
[24] Ngai KL. J Phys Condens Matter 2003;15:S1107.
[25] Roland CM, Schroeder MJ, Fontanella JJ, Ngai KL. Macromolecules 2004;37:2630.
[26] Ngai KL, Beiner M. Macromolecules 2004;37:8123–7.
[27] Beiner M, Ngai KL. Macromolecules 2005;38:7033.
[28] Colmenero J, Arbe A, Coddens G, Frick B, Mijangos C, Reinecke H. Phys Rev Lett 1997;78:1928.
[29] Bergman R, Alvarez F, Alegria A, Colmenero J. J Non-Cryst Solids 1998;235–237:580.
[30] Beiner M, Huth H. Nat Mater 2003;2:595.
[31] Plazek DJ, Ngai KL. Macromolecules 1991;24:1222.
[32] Böhmer R, Ngai KL, Angell CA, Plazek DJ. J Chem Phys 1993;99:4201.
[33] Ngai KL, Plazek DJ. Rubber Chem Technol 1995;68:376.
[34] Floudas G, Placke P, Stepanek P, Brown W, Fytas G, Ngai KL. Macromolecules 1995;28:6799.
[35] Beiner M, Huth H, Schröter K. J Non-Cryst Solids 2001;279:126.
[36] Ngai KL, Habasaki J, Hiwatari Y, Leon C. J Phys Condens Matter 2003; 15:S1607–32; Ngai KL, Habasaki J, Leon C, Rivera A. Z Phys Chem 2005;219:34–42.
[37] Ngai KL. Philos Mag B 2002;82:291.
[38] Wübbenhorst M, Murray CA, Dutcher JR. Eur J Phys E 2003;12:S109.
[39] Scheidler P, Kob W, Binder K, Parisi G. Philos Mag B 2002;82:283.
[40] Rizos AK, Ngai KL. Macromolecules 1998;31:6217–25.
[41] Reissig S, Beiner M, Zeeb S, Höring S, Donth E. Macromolecules 1999; 32:5701.
[42] Schröter K, Reissig S, Hempel E, Beiner M. From small molecules to polymers: relaxation behavior of *n*-butyl methacrylate based systems, unpublished.
[43] Kahle S, Korus J, Hempel E, Unger R, Höring S, Schröter K, et al. Macromolecules 1997;30:7214.
[44] Ngai KL. Macromolecules 1999;32:7120.
[45] Alves NM, Gomez Ribelles JL, Gomez Tejedor JA, Mano JF. Macromolecules 2004;37:3735–44; Salmeron Sanchez M, Gallego Ferrer G, Torregrosa Cabanilles C, Meseguer Duenas JM, Monleon Pradas M, Gomez Ribelles JL. Polymer 2001;42:10071.
[46] Menissez C, Sixou B, David L, Vigier G. J Non-Cryst Solids 2005; 351:595.
[47] Hall DB, Hooker JC, Torkelson JM. Macromolecules 1997;30:667.
[48] Johari GP, Powers G, Vij JK. J Chem Phys 2002;116:5908–12; 2002, 117, 1714.
[49] Paluch M, Roland CM, Pawlus S, Ziolo J, Ngai KL. Phys Rev Lett 2003; 91:115701.
[50] Ngai KL, Casalini R, Capaccioli S, Paluch M, Roland CM. J Phys Chem 2005;109:17356.
[51] Gopalakrishnan TR, Beiner M. J Phys Conf Ser 2006;40:67.